Electronic Supplementary Information

Synergistic Vertical Graphene Skeleton and S-C shell to Construct High-performance $TiNb_2O_7$-based Core/Shell Arrays

Shenghui Shen,[a] Weihao Guo,[a] Dong Xie,[b] Yadong Wang,[c] Shengjue Deng,[a] Yu Zhong,[a] Xiuli Wang,[a] Xinhui Xia,[a] Jiangping Tu [a]*

[a.]State key Laboratory of Silicon Materials, Key Laboratory of Advanced Materials and Applications for Batteries of Zhejiang Province, School of Materials Science & Engineering, Zhejiang University, Hangzhou 310027, China. E-mail: helloxxh@zju. edu.cn;

[b.]Guangdong Engineering and Technology Research centre for Advanced Nanomaterials, School of Environment and Civil Engineering, Dongguan University of Technology, Dongguan 523808, China.

[c]School of Engineering, Nanyang Polytechnic,569830, Singapore

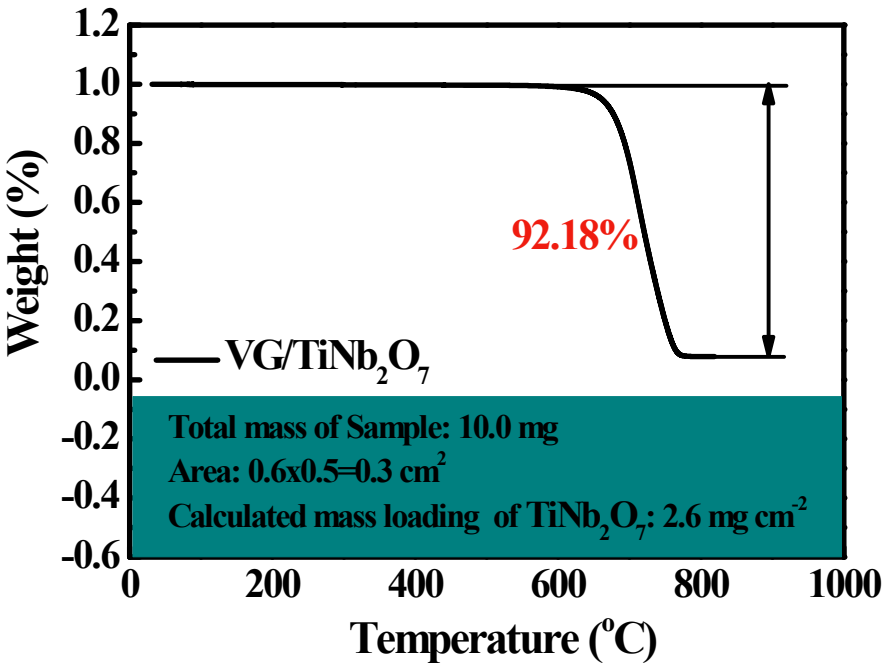

Fig. S1 Thermogravimetric curve of the VG/$TiNb_2O_7$ electrode.

For the TG test, the adopted VG/$TiNb_2O_7$ sample had a total weight of 10.0 mg with a size of ~0.3 cm^{-2}. According to the TG data, the $TiNb_2O_7$ accounted for about 7.82 wt. %. Thus, the mass loading of $TiNb_2O_7$ was ~2.6 mg cm^{-2}.

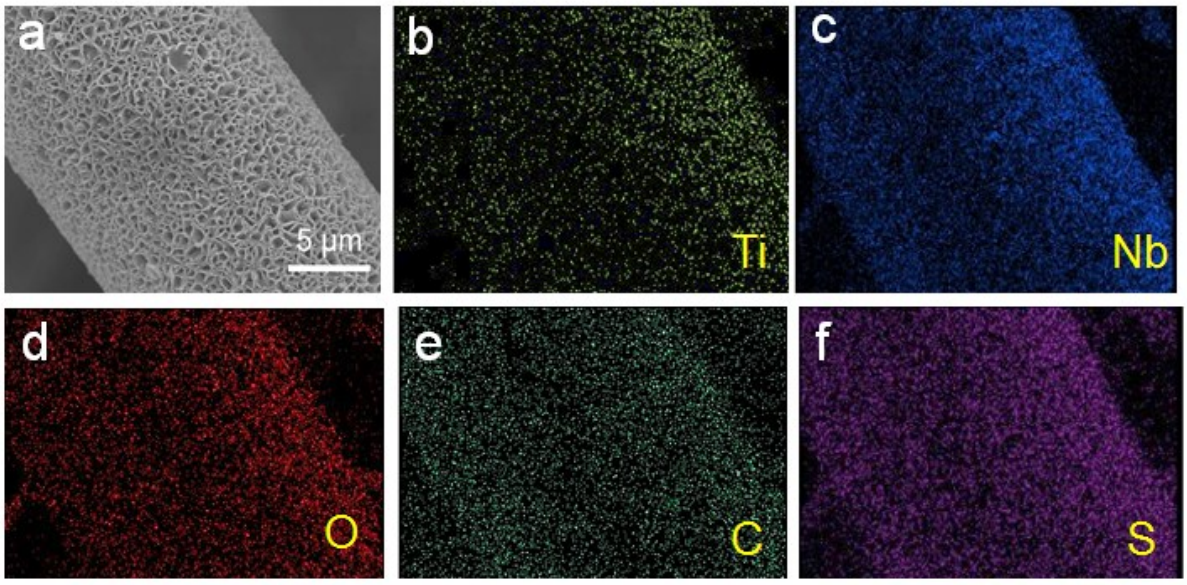

Fig. S2 EDS elemental mapping images of Ti, Nb, O, C, S for VG/$TiNb_2O_7$@S-C arrays.

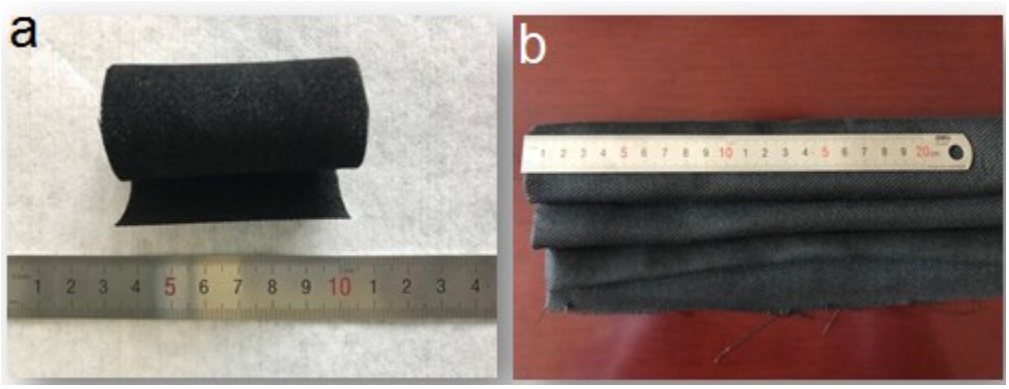

Fig. S3 Photos of VG/$TiNb_2O_7$@S-C electrodes with different sizes.

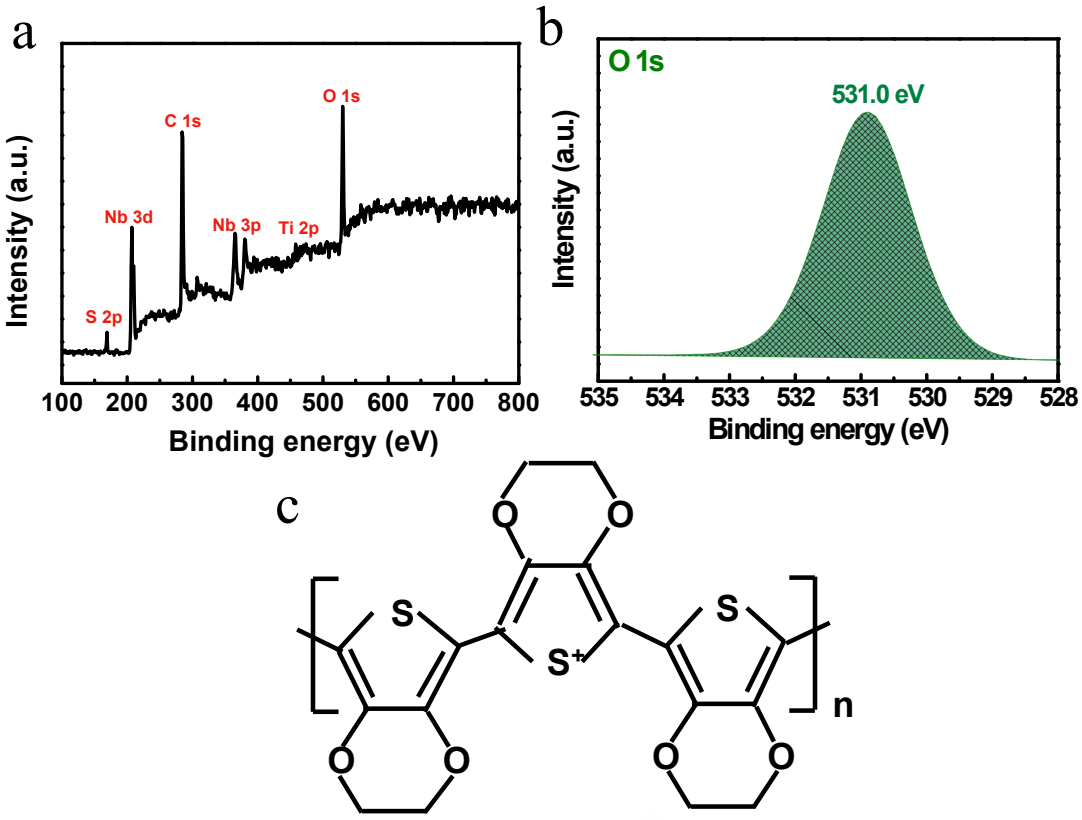

Fig. S4 XPS spectra: (a) Wide-scan survey spectrum, (b) O 1s spectrum of VG/$TiNb_2O_7$@S-C arrays. (c) Molecular structural formula of PEDOT.

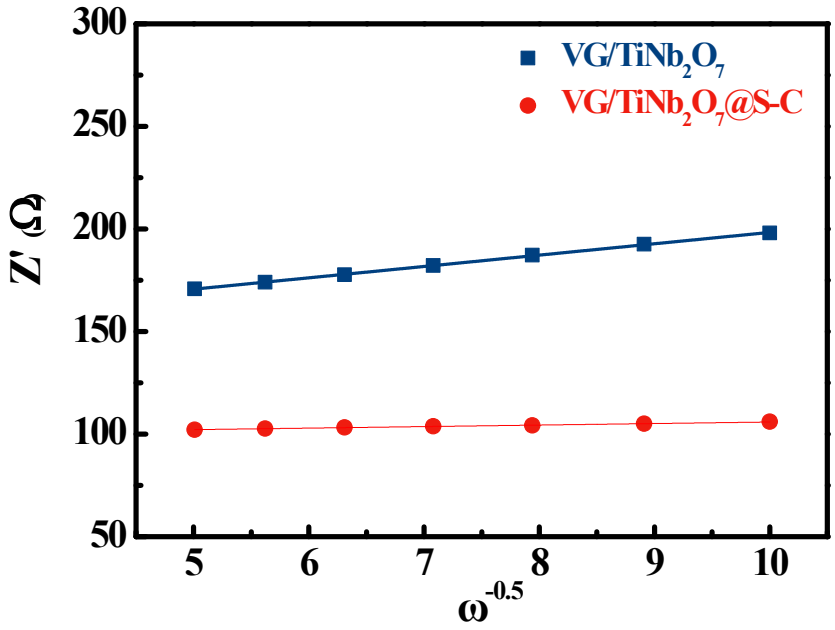

Fig. S5 Z_0–$\omega^{-0.5}$ plots of VG/$TiNb_2O_7$ and VG/$TiNb_2O_7$@S-C samples in the low frequency range at room temperature.

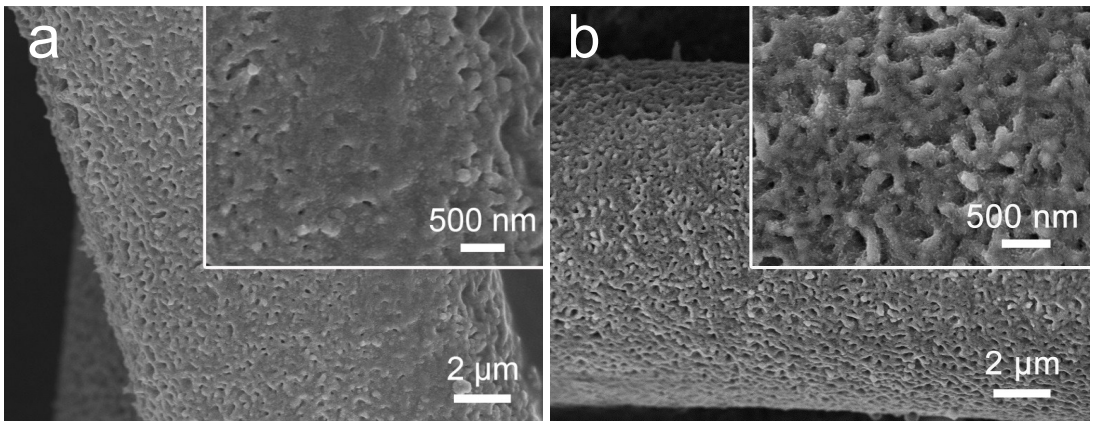

Fig. S6 SEM images after 5000 cycles at 10C: (a) VG/$TiNb_2O_7$ and (b) VG/$TiNb_2O_7$@S-C arrays at 25 °C.

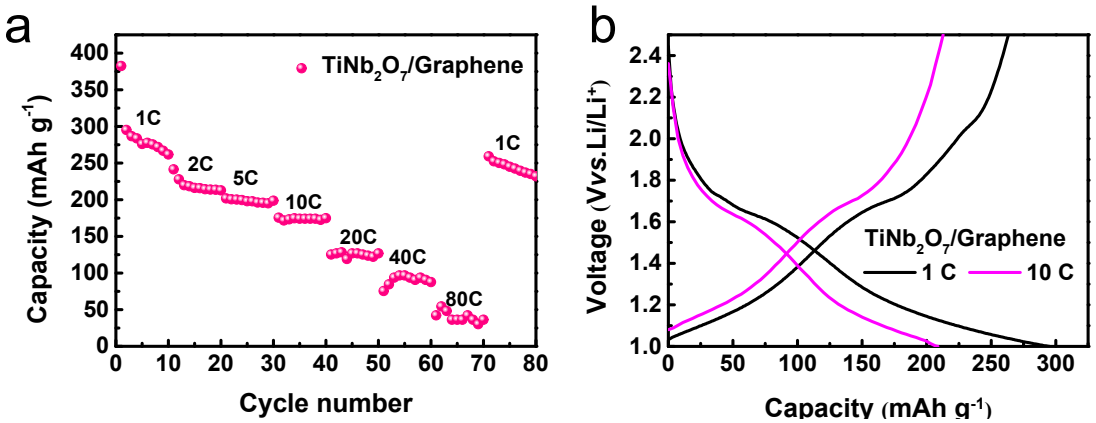

Fig. S7 Electrochemical properties of $TiNb_2O_7$/Graphene electrode: (a) Rate capacities and (b) Charge/discharge profiles at 1 C and 10 C.

The $TiNb_2O_7$/Graphene electrodes deliver capacities of 280 mAh g^{-1} at 1 C and 50 mAh g^{-1} at 80 C, respectively. The capacity of the $TiNb_2O_7$/Graphene electrodes can be recovered to 250 mAh g^{-1} at 1 C.

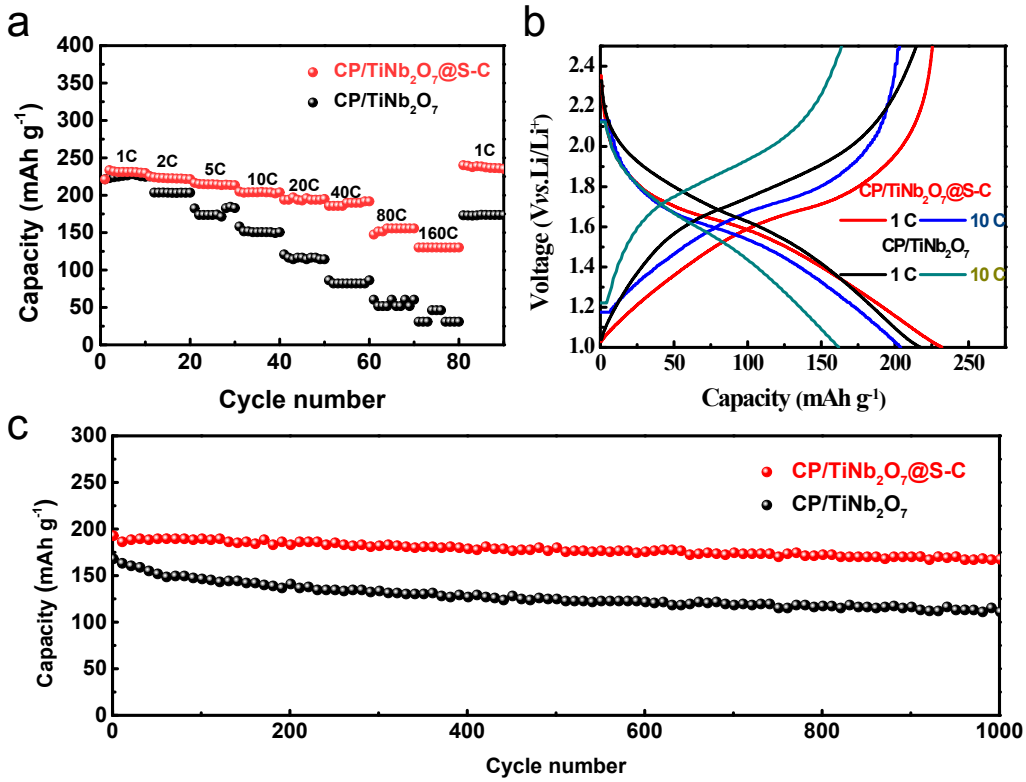

Fig. S8 Electrochemical properties of $CP/TiNb_2O_7$ and $CP/TiNb_2O_7$@S-C electrodes: (a) Rate capacities; (b) Charge/discharge profiles at 1 C and 10 C; (c) Cycling stability at 10 C.

The CP/$TiNb_2O_7$@S-C electrode shows rate performance with a capacity of 230 mAh g^{-1} at 1 C and 130 mAh g^{-1} at 10 C and cycling life with a capacity of 167 mAh g^{-1} at 10 C after 1000 cycles. Apparently, the CP/$TiNb_2O_7$@S-C electrodes exhibit higher rate performance and cycling performance than the CP/$TiNb_2O_7$ counterpart. But the overall electrochemical properties of CP/$TiNb_2O_7$@S-C electrodes are lower than those of the VG/$TiNb_2O_7$@S-C electrodes in this work.

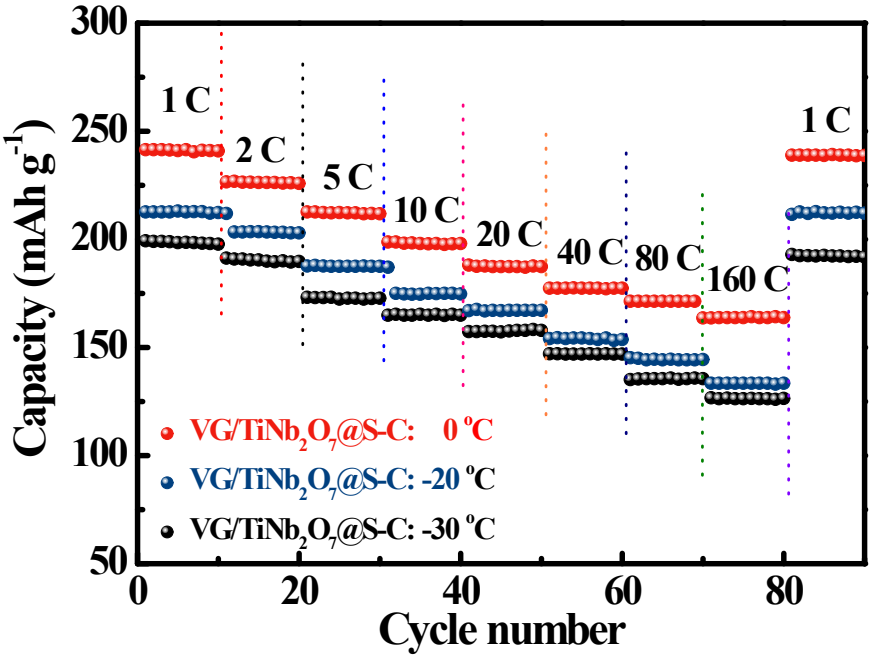

Fig. S9 Rate performance of the VG/$TiNb_2O_7$@S-C electrode at low temperature from 0 to -30 °C.

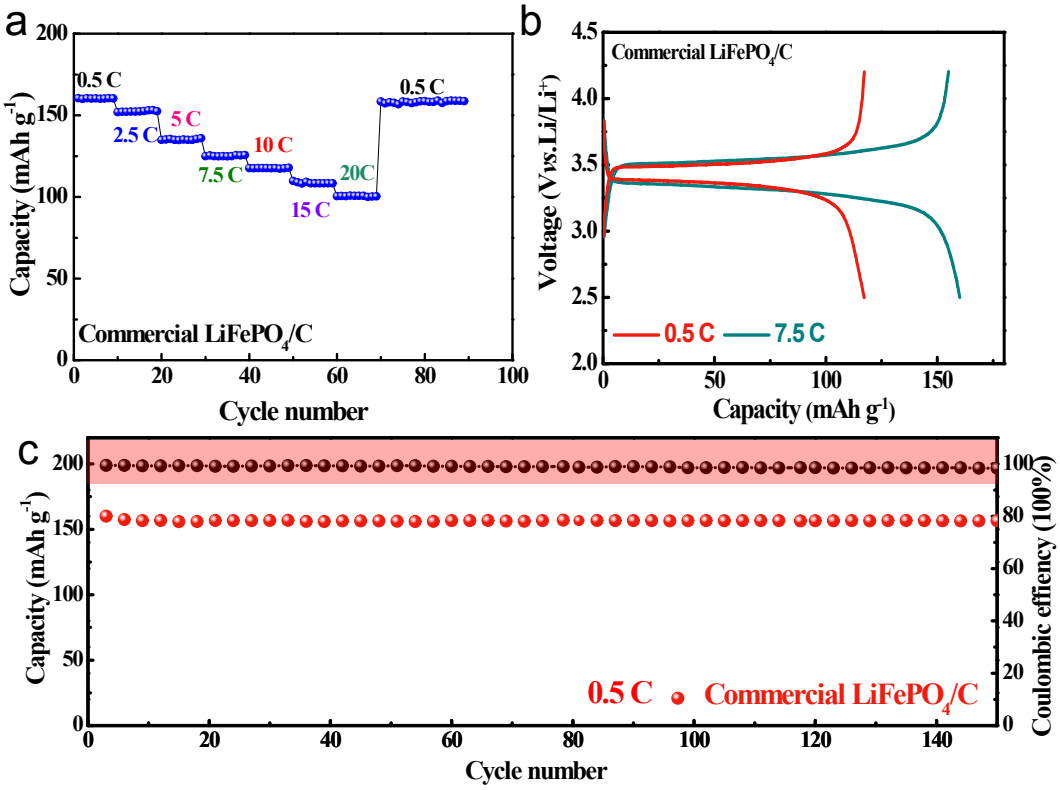

Fig. S10 Electrochemical properties of commercial $LiFePO_4$/C cathode: (a) Rate capacities, (b) Charge/discharge profiles at 0.5 C and 7.5 C, (c) cycling stability at 0.5C.

The commercial $LiFePO_4$/C cathode shows good electrochemical performance with a capacity of 161 mAh g^{-1} at 0.5 C and 119 mAh g^{-1} at 10 C, respectively, as well as good cycling life with a capacity of 156 mAh g^{-1} at 0.5 C after 150 cycles.

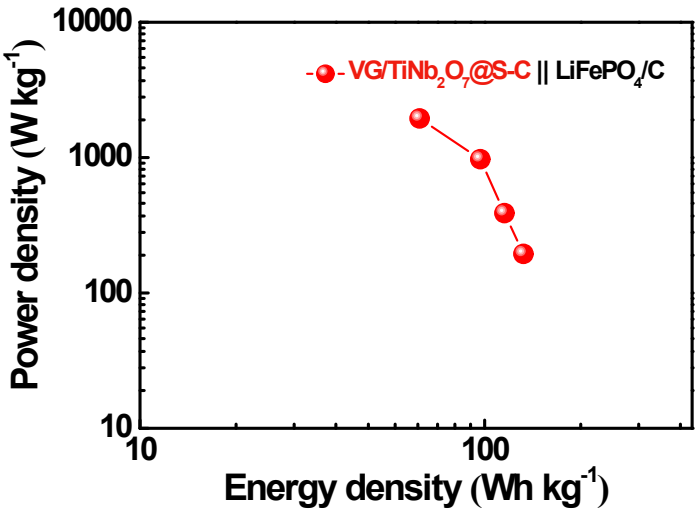

Fig. S11 Ragone plot of the $VG/TiNb_2O_7$@S-C//$LiFePO_4$ full cell.

Table S1. Simulated EIS results of $VG/TiNb_2O_7$ and $VG/TiNb_2O_7$@S-C arrays at room temperature (25 °C).

Electrode	Temperature/°C	R_s (Ω)	R_f (Ω)	R_{ct} (Ω)	D_{Li}(Ω)
$VG/TiNb_2O_7$	25	6.2	43.2	90.5	3.08×10^{-18}
$VG/TiNb_2O_7$@S-C	25	5.4	35.9	35.5	1.59×10^{-16}

Table S2. Rate comparison with other $TiNb_2O_7$-based electrodes

Electrodes	Current density	Specific capacity	Ref.
"Nano-Pearl-String" $TiNb_2O_7$	10 C	140	1
nanostructured $TiNb_2O_7$	50 C	83.9	2
$TiCr_{0.5}Nb_{10.5}O_{29}$/CNTs	20 C	206	3
$TiNb_2O_7$/C microspheres	30 C	120	4
Nitridated PTNO (NPTNO)	100 C	143	5
$TiNb_2O_7$ Nanospheres	50 C	167	6
$Ru_{0.01}Ti_{0.99}Nb_2O_7$	5 C	181	7
3DOM-$TiNb_2O_7$	100 C	99	8
$TiNb_2O_7$ nanotubes	50 C	230	9
$TiNb_2O_7$ hollow nanofiber	10 C	158.4	10
Mo- $TiNb_2O_7$	100 C	180	11
VG/$TiNb_2O_7$@S-C	**160 C**	**182**	**This work**

Table S3. Comparison of the decay rate of other $TiNb_2O_7$-based electrodes

Electrodes	Current density	Decay rate (per cycle)	Ref.
Nano-Pearl-String $TiNb_2O_7$	1C	0.16%	1
Nanostructured $TiNb_2O_7$	10 C	0.078%	2
$TiCr_{0.5}Nb_{10.5}O_{29}$/CNTs	10 C	0.05%	3
$TiNb_2O_7$ /C composite microspheres	5 C	0.11%	4
Nitridated PTNO (NPTNO)	5 C	0.01%	5
$TiNb_2O_7$ Nanospheres	5 C	0.0036%	6
$Ru_{0.01}Ti_{0.99}Nb_2O_7$	5 C	0.099%	7
3DOM-$TiNb_2O_7$	10 C	0.018%	8
$TiNb_2O_7$ nanotubes	1 C	0.02%	9
$TiNb_2O_7$ hollow nanofiber	10 C	0.021%	10
$TiNb_2O_7$ nanorods	10 C	0.09%	12
V- $TiNb_2O_7$	10 C	1.07%	13
VG/$TiNb_2O_7$@S-C	**40 C**	**1.09%**	**This work**

Table S4. Rate capacities of CP/$TiNb_2O_7$ and CP/$TiNb_2O_7$/S-C electrodes

Electrode	1 C	2 C	5 C	10 C	20 C	40 C	80 C	160 C
	mAh g^{-1}							
CP/$TiNb_2O_7$	224	203	173	150	116	82	52	31
CP/$TiNb_2O_7$@S-C	230	222	214	204	194	185	155	130
VG/$TiNb_2O_7$@S-C	284	272	260	248	238	224	205	181

Table S5. Rate capacities of VG/$TiNb_2O_7$@S-C electrode at different temperatures

Electrode	T/℃	1 C	2 C	5 C	10 C	20 C	40 C	80 C	160 C
		mAh g^{-1}							
VG/$TiNb_2O_7$@S-C	25	284	272	260	248	238	224	205	181
	50	338	323	297	279	265	243	229	211
	70	354	333	313	291	276	261	252	241

Table S6. Simulated EIS results of the VG/$TiNb_2O_7$@S-C at medium-high temperature.

Sample	T/°C	R_s (Ω)	R_f (Ω)	R_{ct} (Ω)	D_{Li}(Ω)
	25	5.4	35.9	35.5	1.59×10^{-16}
VG/$TiNb_2O_7$ @S-C	50	3.5	8.6	26.7	2.80×10^{-16}
	70	3.0	3.9	20.7	1.88×10^{-16}

References

[1] K. Tang, X. Mu, P. A. van Aken, Y. Yu and J. Maier, Adv Energy Mater, 2013, 3, 49-53.

[2] S. Lou, Y. Ma, X. Cheng, J. Gao, Y. Gao, P. Zuo, C. Du and G. Yin, Chem Commun 2015, 51, 17293-17296.

[3] L. Hu, R. Lu, L. Tang, R. Xia, C. Lin, Z. Luo, Y. Chen and J. Li, J Alloys Compd, 2018, 732, 116-123.

[4] G. Zhu, Q. Li, Y. Zhao and R. Che, ACS Appl Mater Interfaces, 2017, 9, 41258-41264.

[5] H. Park, H. B. Wu, T. Song, X. W. David Lou, U. Paik, Adv. Energy Mater. 2015, 5, 1401945.

[6] Q. Cheng, J. Liang, Y. Zhu, L. Si, C. Guo and Y. Qian, J Mater Chem A, 2014, 2, 17258-17262.

[7] C. Lin, S. Yu, S. Wu, S. Lin, Z.-Z. Zhu, J. Li and L. Lu, J Mater ChemA, 2015, 3, 8627-8635.

[8] L. Fei, Y. Xu, X. Wu, Y. Li, P. Xie, S. Deng, S. Smirnov and H. Luo, Nanoscale, 2013, 5, 11102-11107.

[9] S. Lou, X. Cheng, Y. Zhao, A. Lushington, J. Gao, Q. Li, P. Zuo, B. Wang, Y. Gao, Y. Ma, C. Du, G. Yin and X. Sun, Nano Energy, 2017, 34, 15-25.

[10] H. Park, D. H. Shin, T. Song, W. I. Park and U. Paik, J Mater ChemA, 2017, 5, 6958-6965.

[11] H. Yu, H. Lan, L. Yan, S. Qian, X. Cheng, H. Zhu, N. Long, M. Shui and J. Shu, Nano Energy, 2017, 38, 109-117.

[12] H. Song and Y.-T. Kim, Chem Commun 2015, 51, 9849-9852.

[13] X. Wen, C. Ma, C. Du, J. Liu, X. Zhang, D. Qu and Z. Tang, Electrochim Acta, 2015, 186, 58-63.